Reply to reviewers comments on "Infrared limb emission measurements of aerosol in the troposphere and stratosphere"

General remarks

We thank the reviewers and the editor for their patience waiting for the replies and the revised version. We thank both reviewers for their helpful and constructive comments. We addressed all comments and suggestions in the reply and have taken them into account in the revised version of the manuscript. We think that this led to a significantly improved version of our manuscript. We hereby confirm that all authors listed on the manuscript agree with submission of the paper in its revised form.

Below you find the original comments of the reviewers in *italics* and our response. Also the changes in the revised version of the manuscript in response to the comments received are shown in sans serif.

Reply to Reviewer 1

Note: In this review I will refer to the author team together as "auth."

Review Synopsis

This manuscript addresses a very important topic in the study of the upper troposphere and lower stratosphere (UTLS), the satellite remote sensing of aerosol and the challenge/promise of aerosol type attribution. Auth make the case clearly that their objective is to treat both sides of the tropopause with equal fidelity. The UTLS is important for climate sensitivity (e.g. Solomon et al. (2011)) yet it is still a frontier of sorts because it represents a local minimum in accurate global measurements and because it is routinely occupied by water-ice clouds, which are confounding in terms of characterization and cloud/aerosol typing. Moreover, the true aerosol/cloud composition of the UTLS involves a rich mix of processes responsible for determining the gaseous and particulate profile, from (for example) in situ particle formation to eruptive/impulsive events like cumulonimbus convection and volcanic activity. Hence studies such as this are critically important and perfectly suited for AMT. Auth are building on a foundation of MIPAS-related cloud and aerosol typing, and working their way down from the "free" stratosphere into the more complicated UTLS. The methods and results they report on here appear to show advances in MIPAS aerosol detection and classification. The approach, combining a theoretical and observation framework, is appropriate and good. In particular, the finding that they can discern vertically resolved water-ice, volcanic ash, and volcanic sulfate in the UTLS merits publication. However, because the global UTLS particulate composition is vastly more complex than this limited array, this work leaves important questions unaddressed and unresolved. Two examples illustrate the point. Mineral dust is known to be in residence at upper tropospheric altitudes (e.g. Husar (2001)). Forest fire smoke is episodically injected into the UTLS (Fromm et al., 2010). It is true that MIPAS has sampled several such events. For this paper to merit publication in AMT, a state-of-the-science accounting of the various UTLS particle types must be acknowledged and the impact of these particle types on MIPAS remote sensing must be addressed. In its current form, this manuscript falls short of this standard. Consequently, I recommend substantial additions before it can be accepted for publication in AMT.

I found myself unable to understand large portions of sections 3.1 and 3.2, on the method for aerosol detection and classification. My difficulty had

to do with the sections' logic, clarity, and internal consistency. Since this represents the core of this AMT candidate, I suggest substantial rework to these parts before the paper can be accepted for publication. Details of my concerns will follow.

Next I will list the major, then minor concerns with the manuscript.

Major:

In the Introduction auth review the omnipresence of aerosol in the climate system. But they leave out some potentially important aspects of UTLS aerosols such as mineral dust presence in the uppermost troposphere (e.g. Husar et al., 2001; Cottle etal., 2013; Liu et al., 2013), upper tropospheric non-volcanic sulfates (Clarisse et al., 2012), and UTLS smoke (e.g. Fromm et al.,2010). To the extent that these and other particle types are likely present in the MIPAS record, it is essential to account for all UTLS pathways in the motivation for this paper.

We agree and added to the introduction: In the upper troposphere and lower stratosphere (UTLS) a large variety of aerosol particles, comprising sulfate droplets, volcanic ash, mineral dust, wild fire aerosol, organic material, and meteoritic dust, have been found (e.g. Junge et al., 1961; Mossop, 1964; Prata, 1989a; Murphy et al., 2007; Fromm et al., 2010; Liu et al., 2013; Weigel et al., 2014).

UTLS dust, smoke, and aerosols other than volcanic ash and sulfates are not included in the aerosol classification part of this paper. Given that the UT aerosol classification is a strong focus of this paper, it could be argued that dust, smoke, and anthropogenic pollution events dominate volcanic perturbations. Either they should be part of the scope of this work or auth need to expressly acknowledge/justify their exclusion.

This paper presents a method to separate between ice clouds and aerosol. To make this point clearer, we changed the term 'classification between ice and aerosol' to 'separation between ice clouds and aerosol' throughout the paper. We added the following sentences to the introduction: Separating between aerosol and ice clouds constitutes the first step towards altitude resolved IR limb emission aerosol measurements in the UTLS. Here, we present a method to detect clouds and aerosol in the troposphere and stratosphere and to separate between aerosol and ice clouds for infrared limb emission measurements. The paper describes the method and shows examples for altitude resolved aerosol detection for three volcanic eruptions at polar, midlatitude and tropical latitudes.

To motivate the choice of volcanic eruptions for the examples we also added

references, which found volcanic aerosol as a main contributor to changes in UTLS aerosol, to the first paragraph of the introduction. The stratospheric aerosol is dominated by sulfate aerosol (Junge et al., 1961) and is significantly influenced by volcanic eruptions (e.g. Bauman et al., 2003; Vernier et al., 2011). Lidar measurements indicate that volcanic aerosol also can be a strongly variable load in the upper troposphere (Di Pierro et al., 2013, Fig. 12).

Section 3.1: I describe below the details of my overall major concern with this section. Some of the items within this description can be considered minor but they are all together to make my point.

I don't understand how selecting a second window band, to distinguish AI from CI, is a strategic consideration. CI already has a window band in the denominator. Auth do not give a compelling reason on P4385 for substituting another window band for the 833/cm band in CI. They do state that they are aiming for altitude and seasonal independence, but they do not make the case that the CI's dependence on altitude and season are driven by the 833/cm window radiances. The apparent justification for choosing 960/cm is given in a new paragraph on P4386. If this is indeed the reason, it should be presented up front where auth are discussing the potential weaknesses of the 833/cm denominator. Moreover, it is not clear to me that the 833-960/cm spectral difference in the water vapor continuum is sufficiently substantial to provide the aerosol clarification needed. Because the continuum is invoked, it would be important to provide more detail or citations to make the point.

We changed the order of arguments and included a reference that shows the changes in water vapour continuum absorption between 8 and 12 μm. The CI detection threshold depends on altitude, latitude, and season, mainly because of the water vapour continuum contributing to the 833 cm^{-1} window radiance (Spang et al., 2004; Sembhi et al., 2012). The effect of the water vapour continuum is particularly pronounced at lower tropospheric altitudes. Because the water vapour continuum absorption decreases with higher wavenumber (e.g. Roberts et al., 1976), we looked for additional windows at higher wavenumbers in MIPAS band A in order to achieve an altitude, latitude and season independent aerosol detection. For the selection of an appropriate window, which cannot be directly adopted from IR nadir measurements due to the strong trace gas emission lines measured in the IR limb geometry, we considered MIPAS clear air radiance profiles between about 7 and 25 km altitude.

On P4386 auth present Figure 2 to illustrate the CI/AI differences. I had a very difficult time understanding the figure and attendant discussion. On L8

auth state that "For regions with CI<2 there are certainly ice clouds..." To what do they attribute this certainty? They seem to be presuming that CI<2 is proof of ice. If this is the case, it is illogical given that the purpose here is to assess the accuracy of CI and AI against some objective truth (cirrus, other clouds, volcanic sulfate, and other aerosols in this post-Nabro orbit). It would be more appropriate here to present some independent evidence of clouds, aerosols, clear sky with which to assess MIPAS UTLS signals. The reader has no information on the true curtain of particles here. A similar presumption based on MIPAS indices is in L11, "For the AI we see that in clear air regions the AI remains above 7." Again, the reader does not know the truth about these scenes (i.e. whether or not that region really is clear) and presumably the intent should be to judge how truthful/accurate the CI and AI are with respect to independent information. On L15, following the discussion of Figure 2 (1 orbit of MIPAS data), auth state that an AI threshold of 7 was discerned based on a visual inspection of all MIPAS orbits in 2011. They present no objective basis on which to assess aerosol/clear-sky boundaries in 2011. In my opinion, the method described here is vague and unsupportable.

In order to make Figure 2 and the process of the ACI threshold estimation more understandable, we restructured Section 3.1. We now start describing how the threshold was derived from simulations and compare then with MIPAS CI aerosol/cloud detections. One important point is that we consider the CI as the accepted and validated method for aerosol and cloud detection for MIPAS. In addition we provide further information on the CI and AI/ACI in the Appendix (A1 – A2). The relevant paragraphs in the manuscript read now:

For the detection of aerosol and clouds along a MIPAS orbit we mainly rely on the established CI. Here we briefly discuss the purposes and shortcomings of the different CI thresholds for the example of a particular MIPAS orbit (Fig. 2b). A fixed CI threshold of 1.8 (CI below 2 shown in yellow) is used for cloud clearing for trace gas profile retrievals by ESA (Spang et al., 2004). This threshold captures tropospheric clouds only and PSCs in the Antarctic, but not a volcanic aerosol layer in the northern hemisphere UTLS as the one caused by Nabro. Also, a fixed CI threshold of 4.5 (yellow, orange, red), which is used for more conservative cloud filtering, mainly captures PSCs (Höpfner et al., 2009), subvisible cirrus clouds (SVCs) (Spang et al., 2015) and tropospheric clouds, but not the volcanic aerosol layer. A fixed CI threshold of 6 (yellow, orange, red, dark red),

captures the UTLS aerosol layer, but mistakes cloud-free regions (profiles 0 – 3, 56 – 60 and 92 – 95, see comparison with IR nadir data below) as cloudy. This feature of the CI of getting smaller at lower altitudes in cloud free conditions is addressed by Sembhi et al. (2012), providing a variable CI threshold definition at altitudes above 10 km. Here we used a simplified variable CI threshold based on Sembhi et al. (2012). The details are given in Appendix A1. This most advanced CI threshold definition (black crosses) allows cloud and cloud free tropospheric regions as seen by IR nadir instruments (Fig. 2f) to be discriminated and captures the UTLS aerosol layer as observed by OSIRIS.

In order to derive a fixed ACI threshold value that is applicable to MIPAS measurements, we investigated the behaviour of simulated ACI profiles for clear air conditions in four atmosphere types (northern hemisphere polar winter, polar summer, mid-latitude, equatorial atmosphere (Remedios et al., 2007)) at UTLS altitudes between 5.5 and 19.5 km with a 0.5 km vertical sampling (Fig A2). We found in the simulations that the ACI is always larger than 7 in the polar winter atmosphere. In the polar summer and mid-latitude atmosphere the ACI is larger than 7 at 7 km and above and in the equatorial atmosphere it is larger than 7 at 9 km and above. This means that a fixed ACI value of 7 would be applicable to MIPAS measurements between 2005 to 2012, after the modification of the measurement geometry in 2005.

Fig. 2 suggests that a fixed ACI with values smaller than 7 captures tropospheric clouds as well as the stratospheric aerosol layer caused by the Nabro eruption. Hence, we assessed the performance of the ACI with a fixed threshold value of 7 for the detection of aerosol and clouds by comparing the ACI aerosol/cloud detections with CI cloud detections relying on the thresholds presented by Sembhi et al. (2012) for altitudes above 10 km and a fixed CI threshold of 2 at 10 km and below (black crosses in Fig. 2b and d). In Fig. 2b and d the profiles 0 – 3, 56 –60 and 92 – 95 are identified as clear air by both the CI and the ACI. The UTLS aerosol layer is also captured by both. However, the CI and the ACI cloud/aerosol detections are not completely identical. Below 10 km the CI with a threshold of 2 identifies slightly less clouds than the ACI with a threshold of 7. Examples can be found in profiles 16, 18, 19 around 10 km and between profile 30 to 40, where the CI detects clear air down to the lowest tangent altitude, whereas the ACI indicates clouds at the lowest tangent altitude. Above 10 km there are a few profiles where the CI identifies clouds/aerosol but not the ACI and vice versa (e.g. profiles 5, 54, 41 – 44). Yet, the main differences can be seen in profiles 16 – 18, where the CI indicates clouds/aerosol down to the tropopause whereas

the ACI indicates a stratospheric aerosol layer with clear air below, and between profile 23 – 35, where the CI indicates a thin stratospheric aerosol layer whereas the ACI indicates aerosol down to the tropopause.

In addition, to address the point of comparing with independent data, we show that both, the MIPAS CI and ACI method are consistent with geostationary IR nadir measurements of upper tropospheric clouds along the discussed orbit. We revised Fig. 2 to also show the IR nadir data.

The tropospheric aerosol/cloud detections of the CI and ACI are confirmed by geostationary IR nadir measurements by MTSAT (15 UTC), IODC (18 UTC) and GOES East (15 UTC) (the IR nadir images were obtained from NERC Satellite Receiving Station, Dundee University, Scotland, http://www.sat.dundee.ac.uk/) along the orbit track (Fig. 2f) and closest to the MIPAS measurement time (15:05 – 16:45 UTC). In the IR nadir images clear air is indicated by dark/black colours, high altitude clouds are bright white and low altitude clouds are indicated by greyish colours. For the clear air profiles 0 – 2 north west of Australia (22 – 20° S), 53 – 60 west of South America (2° N – 23° S) and 92 – 95 over the Indian Ocean the IR nadir images show only low altitude clouds, which are below the lowest tangent altitude of MIPAS. Over Asia (7° S – 15° N) many high altitude clouds are present (profiles 4 – 15). Over north China and Mongolia there is a gap in the high altitude clouds (profiles 17 – 18). Over north and central America (10 – 60° N) there are patchy cloud patterns, which is also reflected in the alternating cloudy and clear air profiles (profiles 38 – 51) measured by MIPAS. From 26 – 60° S (profiles 61 – 70) there is a large field of high altitude clouds. At latitudes higher than 60° the results from geostationary images become uncertain, hence they are not discussed here. A detailed assessment of the detection sensitivity and altitude information accuracy of the MIPAS measurements of the UTLS aerosol layer will be presented in a future study.

Figure 2 was difficult for me to interpret. Even though latitudes and longitudes are given, I would suggest a map panel be presented so the reader can easily see where in the world this orbit was. The color difference between important index thresholds (e.g. AI=7) was not stark enough for easy feature discernment. Moreover, there is no tropopause information on the plot, hence it is difficult to assess the UTLS. A tropopause line would help this figure enormously. Auth point out some features in Figure 2 that I could not unambiguously identify. For instance the "detached layer" (L13) is murky to my eye. Perhaps auth could annotate the figure with arrows or some such device to make these specific features readily identifiable.

We added a map panel to Figure 2 and the tropopause. The tropopause very much helps to identify the stratospheric aerosol layer. We also improved the colour scale and checked that it is also suited for red-green colour blind. Because the CI and ACI are continuous indices, we refrained from introducing a pronounced colour difference at the ACI of 7. ACI values smaller than 7 are shown in yellow and shades of red and ACIs larger than 7 are shown in shades of blue. To the figure caption we added:

White curves in **b** to **e** denote the thermal tropopause according to the World Meteorological Organization (WMO) definition along the orbit track derived from ERA-Interim data (Dee et al., 2011). In polar winter the thermal tropopause often is not present (Zängl and Hoinka, 2001).

P4386, 2nd paragraph. The discussion of the compromised behavior of AI above 25 km is important but is not supported well. Auth refer to Figure 1 while discussing artifacts above 25 km, which is the top of Fig. 1. I.e. it's difficult to know what the reader is supposed to see in Fig. 1 to understand the issue. Please either clarify the discussion or increase the altitude range of Figure 1.

We added a Fig. A1 to the Appendix (A2) that shows the CI and AI up to 50 km and refer to this figure:

In the stratosphere at altitudes from about 50 km down to about 22 km we found a seasonal and diurnal cycle in the radiances between 960 and 961 cm^{-1} and hence in the AI (Fig. A1).

P4387, L5. Auth state "To further confirm the ACI threshold of 7 we derived. . . " In my assessment, the ACI=7 wasn't confirmed (see my comments above), so a further confirmation is not possible. Perhaps auth mean "evaluate" instead of "further confirm"?

We changed the line of argumentation and rephrased this sentence. We now start with the simulations, derive a threshold from the simulations, apply it to the measurements and compare it to established CI method. We also added a comparison with nadir measurements in Sec. 3.1.3 and simulated profiles of clear air, ice cloud and aerosol scenarios to Appendix A3. Please also see comment above.

P4387, L5-26. Here auth use a radiative transfer model with a module (MT_CKD) that is considered to be inaccurate for real atmospheric conditions to assess their empirical AI=7 clear/aerosol threshold. The simulations are grossly at odds with the MIPAS data. Auth then conclude that their

theoretical approach has uncertain merit, so fall back exclusively on the empirical approach's result. This exercise does not, I my assessment, "further confirm" the ACI threshold. It's not clear to me what good this particular simulation exercise was. I do believe that something in addition to the empirical/visual thresholding is called for. I'd suggest auth either reformulate the RTM strategy or invoke independent aerosol/cloud observations to evaluate the ACI.

We changed the wording to make clear that this scheme causes problems below 7–10 km (polar region to tropics, respectively), but not above. The paragraph above and Figure B2 show that the simulations perform very well for the vast majority of the MIPAS measurements. The paragraph about the limits of the simulations reads now:

For the measurements before 2005 we analyzed also altitudes below 7 – 9 km. For these altitudes the simulations in Sec. 3.1.2 indicated that the ACI for clear air falls below 7 at altitudes below 7 – 9 km. However, we often found ACI values significantly larger than 7 down to the lowest tangent altitudes (Figs. A2, A4) in the MIPAS measurements before 2005. As the most likely reason for the discrepancy between the measurements and simulations below 9 km we identified the water vapour continuum assumed in the simulations. On the one hand we used climatological water vapour profiles that inherently do not cover the complete variability in the atmosphere, and on the other hand in JURASSIC the Mlawer–Tobin–Clough–Kneizys–Davies 1.10 scheme (MT_CKD) (Clough et al., 2005) is used for the water vapour continuum representation. This scheme was found to represent real conditions with insufficient accuracy at lower altitudes (Griessbach et al., 2013). Hence, the ACI has the potential to be also applied to the MIPAS measurements before 2005, where the lowest tangent altitude reached down to nearly 5 km at all latitudes.

Section 3.2: I describe below the details of my overall major concern with this section. Some of the items within this description can be considered minor but they are all together to make my point.

P4388, L3. Auth begin section 3.2.1 discussing their choice of windows "for the discrimination between aerosol and ice clouds." It seems to me that they had already done that in section 3.1. Hence the introduction to this discussion seems to need clarification. On L10 they claim to have identified in Section 3.1 three window regions, yet there is no such attempt in 3.1. Moreover, of the three bands listed, only one (960-961/cm) has roots in 3.1. This makes me wonder if indeed there is material they intended for the AI/CI definition

that was left out of 3.1. Please clarify.

We already had candidate regions for the windows based on the optical properties and studies performed for IR nadir. For the selection of the narrow window boundaries we used the same methodology as described in section 3.1 (visual inspection of measured clear air profiles). To clarify this we rephrased the paragraph. It reads now:

For the separation between aerosol and ice clouds by IR nadir measurements spectral windows around 8.5, 11 and 12 μm (1176, 909, 833 cm^{-1}, respectively) are employed (Ackerman, 1997; Guehenneux et al., 2015). For these windows the optical properties of ice differ most strongly from aerosol such as volcanic ash, soil-derived aerosol and sulfate aerosol (Ackerman, 1997). For the IR limb emission measurements of MIPAS we identified three narrow windows that have very little interference with trace gases and exploit the spectral differences between the optical properties of ice and, in our case, volcanic aerosol.

On P4388 auth expressly limit the aerosol typing that they intend to model and discern as volcanic ash and sulfate. It is here specifically that I would expect auth to either include the full suite of aerosols that MIPAS encounters in the upper troposphere, or to explain why they are limiting the scope to ash and sulfates. If they intend to explore the more representative array or aerosols in future work, this would be the place to make that point.

We did not intend to classify the whole aerosol suite. This paper is rather on the fundamental first step of filtering out ice clouds. We chose volcanic aerosol as a representative of the entire aerosol family for multiple reasons:

- availability of complex refractive indices in IR with sufficient spectral resolution
- UTLS aerosol is dominated by sulfate aerosol and from the MIPAS perspective volcanic eruptions are the most prominent events. We added to the first paragraph of the introduction: The stratospheric aerosol is dominated by sulfate aerosol (Junge et al., 1961) and is significantly influenced by volcanic eruptions (e.g. Bauman et al., 2003; Vernier et al., 2011). and The tropospheric background aerosol is also dominated by sulfate aerosol but is disturbed by numerous irregular events, such as volcanic eruptions, mineral dust outbreaks, and fires. ... Lidar measurements indicate that volcanic aerosol also can be a strongly variable load in the upper troposphere (Di Pierro et al., 2013, Fig. 12).

- the windows we used are particularly suited for volcanic ash, soil-derived aerosol and sulfate aerosol. Hence we added to the text: For these windows the optical properties of ice differ most strongly from aerosol such as volcanic ash, soil-derived aerosol and sulfate aerosol (Ackerman, 1997).

P4389, L11-14. I was confused about these various ranges of numbers and the meaning thereof. It seemed to me that there was a lot of overlap, making it hard to draw any conclusions. I ask auth to provide clarification on how they interpret these ranges of percents.

We pointed out these numbers and ranges to show that scattering really matters, and depends on the particle size, type and the wavenumber. To make this point clearer we added:

The single scattering albedo depends on particle size and wavenumber (Fig. 3d). The scattering contributions range from 30 to 80 % for small ice particles and are nearly constant around 55 % for large ice particles. The scattering contribution of the sulfate aerosol is generally below 10 % and for volcanic ash it ranges from 15 to 80 %. Hence, scattering effects can not be neglected for any particle type discussed here.

P4389, 3.2.2. On L23 auth discuss how they defined "regions where they expected" to find four cloud/aerosol scenarios. They do that by listing broad latitude ranges in Figure 4, but no additional qualification. E.g. there is no longitudinal information that might be logical if they are focusing on a volcanic plume. They give no altitude range selection criteria. In my assessment, this gives too little help to the reader. And if indeed there are no other criteria than in the Figure caption, it seems too broad a selection scope. Hence interpreting the patterns in Figure 4 is met with great uncertainty as to just what the true physical constituents are that are in the plot. One suggestion I have is to segregate data points by their tropopause-relative position. The reader would benefit greatly if he/she could see at a glance where the tropospheric/stratospheric particles and ice are.

We agree that the way we presented the measurements first an then the simulations makes it difficult for the reader to follow and to be convinced. Hence, we changed the order and present now our simulations first (Section 3.2.2) followed by the measurements (Section 3.2.3) and a subsection on the thresholds including the discussion comparing the simulations with the measurements (Section 3.2.4). This way we think the simulations give an

indication on what to expect for ice clouds and the volcanic aerosol. In the measurements the reader will now be able to recognize the specific patterns shown in the simulations. We also give a more detailed description of the measurements (Section 3.2.3) indicating the exact regions and references for each "aerosol event". However, for the measurement figure (now Figure 5) we still apply our method to all longitudes in the corresponding latitude ranges including atmospheric variability and ice clouds by purpose. Our intention is to show that if aerosol is present, it clearly stands out.

Because we rearranged and rewrote the original sections 3.2.2 and 3.2.3 to the new Sections 3.2.2, 3.2.3 and 3.2.4, we refrain from repeating them here and would like to refer to the revised manuscript.

In the above comments I have mentioned my concern for the lack of an independent aerosol/cloud observation data set with which to compare the MIPAS indices. It seems to me that the CALIPSO vertical feature mask, and even CloudSat data, could be put to great use in this application. The time coincidence is not ideal, but for the types of data presented herein (e.g. the global MIPAS curtain 2 months after Nabro) time coincidence is not a strict criterion.

We thought that too, however, concerning the Nabro aerosol in Fig. 2 and Fig. 5b, the daytime CALIPSO backscatter plots and the vertical feature mask do not indicate the Nabro aerosol layer anymore by end-July. In the nighttime CALIPSO backscatter data the layer can be spotted, but in the vertical feature mask it is very patchy (e.g. `http://www-calipso.larc.nasa.gov/data/BROWSE/production/V3-01/2011-07-29/2011-07-29_23-02-18_V3.01_1_1.png` and `http://www-calipso.larc.nasa.gov/data/BROWSE/production/V3-01/2011-07-29/2011-07-29_23-02-18_V3.01_1_6.png`). By mid-August even in the nighttime backscatter data the layer is not visible anymore (e.g. `http://www-calipso.larc.nasa.gov/data/BROWSE/production/V3-01/2011-08-18/2011-08-18_17-39-19_V3.01_1_1.png` and `http://www-calipso.larc.nasa.gov/data/BROWSE/production/V3-01/2011-08-18/2011-08-18_17-39-19_V3.01_1_6.png`).

Since there is a better CALIOP aerosol product than provided on the CALIPSO web page, we initiated a comparison of MIPAS sulfate aerosol detections with the CALIOP nighttime aerosol product (provided by J.-P. Vernier) for the Nabro eruption between June to early August 2011 from 0-50N. In this

comparison we also compare with ground based lidar measurements 50-68N between August 2011 and February 2012, and ground based twilight measurements in August 2011. Since this comparison is beyond the scope of this paper and quite extensive, we decided to present it in a separate paper. Two preliminary examples of the MIPAS comparison with CALIOP are given in Fig. R1.

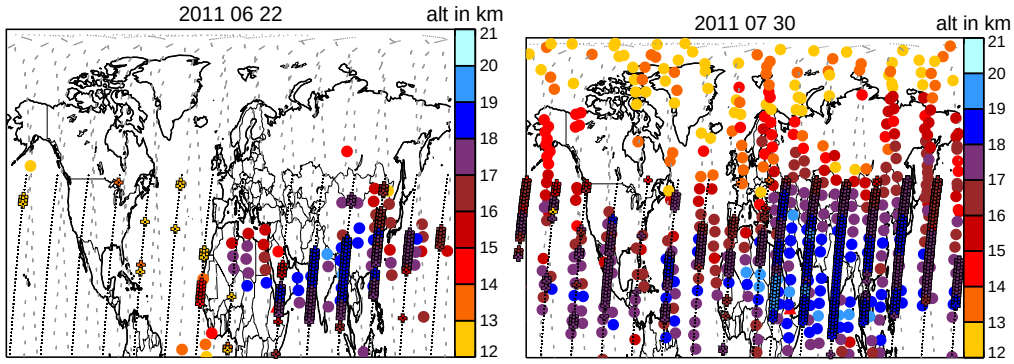

(a) **(b)**

Figure R1: Comparison of aerosol top altitudes measured by MIPAS and CALIOP. The CALIOP aerosol product is only available for nighttime measurements. In June, July, and August the CALIOP nighttime measurements in the northern hemisphere are available between 0 and 50° N. Here we used an extinction of $5\times10^{-3}\,\mathrm{km}^{-1}$ to derive the aerosol top altitude from the CALIOP data. MIPAS day- and nighttime orbits are indicated by grey dashes and MIPAS aerosol detections are indicated by coloured circles. The CALIPSO nighttime orbits are indicated by black dots and the aerosol detections by coloured crosses. **(a)** 22 June **(b)** 30 July.

Regarding the Puyehue aerosol, CALIOP unfortunately did not measure between day 2 to 9 following the initial eruption on 4 June 2011. In addition the aerosol was transported by the jet stream very quickly and hence, in this case time coincidence really matters. For Fig. 5, where we show measurements from 16 June 2011, we compared with CALIOP and found several cases similar to what we observed for the Nabro aerosol: a layer is visible in the backscatter plot and here also in the depolarization ratio plot, but not in the vertical feature mask (e.g.

`http://www-calipso.larc.nasa.gov/products/lidar/browse_`

images/show_detail.php?s=production&v=V3-01&browse_date=2011-06-16&orbit_time=06-53-39&page=2&granule_name=CAL_LID_L1-ValStage1-V3-01.2011-06-16T06-53-39ZN.hdf).

In order to substantiate our assumption that volcanic aerosol is present, we added a reference to Sec. 3.2.3:

For 16 June 2011 (Fig. 5c) we expected to find volcanic ash at latitudes between $0-60^{\circ}$ S originating from the eruption of the Puyehue Cordón-Caulle (Klueser et al., 2013) and ice clouds as well.

Regarding the ice clouds, previous comparisons of MIPAS with CALIOP found that for ice clouds at low and mid-latitudes the match times are not close enough (Hurley et al., 2011). Hence, ice cloud comparisons would only be feasible on a statistical basis. Also, Davis et al. (2010) found that CALIPSO might miss 2/3 of thin cirrus clouds with vertical optical depth <0.01 in its current data products to which IR limb measurements are sensitive to (Spang et al., 2015). The same holds for CloudSat (It is also in the A-train and hence, the matches in time are not sufficient for convective clouds. In addition radar measurements are not sensitive to sulfate aerosol.).

In order to demonstrate that the volcanic aerosol is detected by MIPAS in the right places, we show comparisons with AIRS horizontal high resolution volcanic emission measurements in Sec. 4.

Minor

In the introduction, auth survey prior attempts to retrieve UTLS cloud/aerosol types and promote the advantages of IR limb sensing. No mention is made of the work done with HIRDLS. Sembhi et al. (2012) is cited but not for its use of HIRDLS cloud detections.

We agree that HIRLDS should be mentioned in the introduction. Hence, we added to the 5th paragraph (about IR limb emission aerosol measurements) of the introduction:

Measurements of the High Resolution Dynamics Limb Sounder (HIRDLS) (Gille et al., 2008) provide a flag for four different cloud types in the troposphere and stratosphere ($1-$unknown cloud, $2-$cirrus layer, $3-$extensive PSC, $4-$opaque cloud) and $12\,\mu$m extinctions. HIRDLS measurements are also sensitive towards volcanic aerosol and forest fire smoke clouds, which the detection routine classifies as "unknown cloud" (Massie et al., 2007). However, not only aerosol is classified as "unknown cloud", also multilayer cloud structures and clouds of intermediate thickness between deep convection tower and isolated cirrus layer fall in the

"unknown cloud" category (Massie et al., 2007).

Also in the survey of prior vertically resolved aerosol/cloud retrievals, auth use the term "limb measurements in the IR" or variants thereof, and limit their survey to measurements of IR emission. If this is their intent, they should specify "emission." Otherwise, they leave out several important NIR- and IR-based accomplishments, e.g. HALOE and SAGE (Thomason, 2012).

We agree, hence we added further limb instruments measuring aerosol profiles and a discussion to the introduction:

Satellite based limb instruments, such as the Stratospheric Aerosol and Gas Experiment (SAGE) series (Thomason et al., 1997; Bauman et al., 2003), Optical Spectrograph and InfraRed Imaging System (OSIRIS) (Rieger et al., 2015), and the Halogen Occultation Experiment (HALOE) (Thomason, 2012) have a long standing history of measuring altitude resolved global time series of stratospheric aerosol. However, the spatial coverage of solar occultation instruments (SAGE, HALOE) is limited. The solar scattering (OSIRIS) measurements are limited to daytime and hence cannot provide measurements at polar night. Also, due to the high sensitivity to low aerosol concentrations of these instruments measuring in the ultraviolet to near-infrared spectral range, their extinction profiles run into saturation for specific aerosol events, such as moderate volcanic eruptions (with an volcanic explosivity index (VEI) of 4, e.g. Sarychev 2009, Nabro 2011) and impede measurements below the plume top altitude (Fromm et al., 2014). The 750 nm extinction coefficient thresholds range from about 3×10^{-3} to 0.02 km^{-1} for OSIRIS and SAGE II respectively (Fromm et al., 2014). Extending these aerosol measurements into the upper troposphere is also challenging, because the separation between ice clouds and aerosol is prone to errors for SAGE and HALOE (Kent et al., 2003; Thomason and Vernier, 2013) or is not done for OSIRIS (Fromm et al., 2014).

To be more precise we changed the term "IR limb measurements" to "IR limb emission measurements", where appropriate, throughout the paper.

P4385, L7. Why is the CI cloudy-air threshold expressed as a range? What is the significance of CI-1.8?

We expressed the CI threshold as a range, because different thresholds are used in different publications as cited in the paper. Sembhi et al. (2012) analyzed this in detail and provided altitude, latitude and season dependent thresholds. The next sentence in the manuscript reads:

The CI detection threshold depends on altitude, latitude, and season, mainly

because of the water vapour continuum contributing to the 833 cm^{-1} window radiance (Spang et al., 2004; Sembhi et al., 2012).

We also added the following sentence to the third paragraph of Sec. 3.1:

A fixed CI threshold of 1.8 (CI below 2 shown in yellow) is used for cloud clearing for trace gas profile retrievals by ESA (Spang et al., 2004).

P4389, L22. Auth mention "four selected days" and then "(about 14 orbits)." There are 14 orbits in a single day. So does this mean 14 orbits spread over 4 days? Please clarify and give the dates.

We rewrote the description of Fig. 5 (now):

we show four selected cases of UTLS aerosol measurements in order to verify the simulations (Fig. 5). For each case we used all measurements of an entire day, which is about 14 orbits, in the latitude range given below and at altitudes between MIPAS lowest tangent altitude (about 7 km) and 25 km. For the longitude range we did not introduce a limitation in order to include also clear air and ice clouds.

And then we describe each plot of Fig. 5 in more detail giving the dates.

For 17 May 2011 (Fig. 5a) ...
For 29 July 2011 (Fig. 5b)...
For 16 June 2011 (Fig. 5c)...
For 29 January 2011 (Fig. 5d)...

Figure 4 caption. This is presumably a northern summer period, hence "PSCs (0-90N)" should be 0-90S.

The data in Fig 4d (now 5d) were measured on 29 January 2011, which is northern hemisphere winter.

Figure 4 caption. "All figures comprise ... single day." This is inconsistent with the text "four selected days."

All panels comprise a single day, which are about 14 orbits. Please see comment above, where we improved the description of this Figure.

Figure 6. The height-scale colors provide too little contrast between height bins. Please consider a clearer height differentiation.

We agree that the color are not optimal. We changed them.

We also went through the comments in the commented manuscript and made the suggested changes to the manuscript.

Reply to Reviewer 2

General comments

In this paper the authors have extended the capabilities of MIPAS to discriminate between ice, sulfate aerosol and volcanic ash in the UTLS. Improved methods for height resolved aerosol/cloud detection and discrimination for limb emission sounders and the resulting scientific applications clearly merit publication in AMT. However, the current iteration requires some improvement before it can be accepted for publication. Obviously the paper is concentrating specifically on the limb emission technique, but the substantial background on similar techniques pioneered for nadir sounders should be discussed in appropriate detail. Likewise, investigations of other aerosols present substantially in the UTLS (e.g. mineral dust) have been undertaken for nadir sounding (see reference below) and therefore some discussion of these is warranted.

Improved space borne detection of volcanic ash for real-time monitoring using 3-Band method, Y. Guéhenneux et al, Journal of Volcanology and Geothermal Research 293 (2015) 25–45.
Prata, A.J., 1989a. Observations of volcanic ash clouds using AVHRR-2 radiances. Int. J. Remote Sens. 10 (4–5), 751–761. `http://dx.doi.org/10.1080/01431168908903916`.
Prata, A.J., 1989b. Radiative transfer calculations for volcanic ash clouds. Geophys.Res. Lett. 16 (11), 1293–1296. `http://dx.doi.org/10.1029/GL016i011p01293`.

We changed our wording from "IR limb" to the more precise "IR limb emission" throughout the manuscript. Also, we substantially reworked the introduction and discussed the IR nadir methods in more detail including the suggested references.

In contrast, satellite based infrared (IR) emission measurements provide a global coverage at day- and nighttime during all seasons. Furthermore, IR nadir instruments have a better global and temporal coverage than UV/VIS nadir measurements or occultation measurements. IR nadir measurements have a long standing history in detecting aerosols and retrieving aerosol composition and microphysics. The aerosol measurements from IR nadir instruments mainly focus on volcanic ash (e.g. Prata, 1989a; Guehenneux et al., 2015) and mineral dust (e.g. Peyridieu et al., 2010; Klueser et al., 2011, 2012; Liu et al., 2013). There are several methods available to detect aerosol, filter out ice clouds and to classify aerosol

types. These methods comprise the split window/reverse absorption technique for volcanic ash (Prata, 1989a,b), trispectral approaches for volcanic ash and mineral dust (Ackerman et al., 1990; Ackerman, 1997; Guehenneux et al., 2015), and multispectral approaches for hyperspectral instruments (Gangale et al., 2010; Clarisse et al., 2010, 2013). Although the established methods are used for operational data products they are still subject to improvements (Guehenneux et al., 2015). The capability of detecting sulfate aerosol with IR nadir measurements has been demonstrated for band measurements (Baran et al., 1993; Ackerman, 1997) and for hyperspectral instruments (Clarisse et al., 2010; Gangale et al., 2010; Karagulian et al., 2010). Ackerman (1997) found that sulfate droplets with an aerosol optical depth (AOD) larger than 0.01 at 11 μm (which corresponds to an AOD of about 0.1 in the VIS range for the same scenario) should be detectable from IR nadir measurements.

In Section 3.1 we added the following sentence to point out the differences between IR nadir and IR limb emission measurements regarding the selection of appropriate window regions for aerosol and cloud detection.

For the selection of an appropriate window, which cannot be directly adopted from IR nadir measurements due to the strong trace gas emission lines measured in the IR limb geometry, we considered MIPAS clear air radiance profiles between about 7 and 25 km altitude.

Specific comments

P4832,L11: Some references and deeper discussion is needed here.

We deleted this sentence and wrote:

Aerosol detection and the separation from ice clouds for IR limb emission measurements is by far not as elaborated as for IR nadir measurements.

This sentence is supported by the three paragraphs above, discussing IR nadir and IR limb emission aerosol and cloud detection and classification methods and citing the appropriate references.

P4836,L25: Make it clear clear that the non-LTE effects occur much higher in the atmosphere (>> 25 km) and that the effects on ACI are because the instrument is looking through this NLTE region at the UTLS tangent heights.

We write now:

This diurnal cycle and the differences between the summer and the winter hemisphere are most likely caused by non-local thermodynamic equilibrium (non-LTE) effects of the CO_2 laser bands between 950 and 970 cm^{-1} at altitudes of 50 km and above (e.g. Timofeyev et al., 1995).

P4388, 3.2 Aerosol and Ice Classification. This section is really quite hard to follow. It would be informative to indicate that the imaginary refractive index determines the ir absorption. Suggest calling the 3 spectral regions A,B,C. Maybe replace some of the text with a table or put +/- symbols on Fig 3 to mark the gradient signs.
For example ...
Three spectral columns A,B,C and two rows for Im and Re indices. Then each cell contains + or - (depending on sign of gradient). Ice spectral gradient seems quite flat (?) for Region C. Not sure I got all the signs correct.
A B C Im Ice - - ? SA + + - VA + + -
Re Ice - + ? SA + + + VA + + -

We agree. This paragraph is hard to follow. First, we added the following:

As the imaginary part of the complex refractive index determines the IR absorption and the real part determines the scattering, these differences between ice clouds and aerosol (volcanic ash and sulfate aerosol) propagate to the optical properties (Fig. 3c and d).

Following your suggestions we rewrote and shortened the discussion on the spectral gradients using "positive" and "negative gradient". We think it is now much easier to follow.

The imaginary part of the refractive index (Fig. 3a) has a positive spectral gradient for ash and sulfate between 830 and 960 cm^{-1}, whereas the spectral gradient of ice is negative. Also, between 830 and 1224 cm^{-1} the spectral gradient is positive for sulfate, but negative for ice. For the real part of the refractive indices (Fig. 3b), the spectral gradient between 830 and 960 cm^{-1} is positive for ash and sulfate, but negative for ice. The spectral gradient between 960 and 1224 cm^{-1} is negative for ash and sulfate, but positive for ice.

P4389, 3.2.2 Measurements. This section really needs to discuss previous work on BTDs in nadir view since it's hardly a surprise that BTDs also provide cloud/aerosol discrimination in the longer path limb view.

We agree. We added the following to Section 3.2.2 Simulations:

For IR nadir measurements it is common practice to use brightness temperature differences (BTDs) for the discrimination between volcanic or soil-derived aerosol and ice clouds (e.g. Prata, 1989a; Ackerman et al., 1990; Ackerman, 1997).

and

In contrast to IR nadir BTD correlations that often correlate $11-12\,\mu$m with

$8-11\,\mu$m (e.g. Ackerman et al., 1990; Hong et al., 2010) we found for MIPAS IR limb spectra the clearest correlation patterns for the BTDs between the 830 and 1224 cm^{-1} ($12.0-8.2\mu$m) windows and the 960 and 1224 cm^{-1} ($10.4-8.2\mu$m) windows.

Please note that in response to reviewer 1 we changed the order of the sections to: 3.2.2 Simulations and 3.2.3 Measurements.

P4394,L14: A U-shaped
Done.

P4394,L24 and P4396,L12: Loss rate of SO2 in presence of clouds is faster than gasphase chemistry alone. Is the process oxidation or hydrolysis or both?

In the stratosphere the process is oxidation. In the upper troposphere also oxidation is the dominating process, because mainly ice clouds are present. Liquid water clouds can usually be found at altitudes below about 5 km (Hu et al., 2010) that we do not consider here. Also, from IR measurements SO_2 and sulfate aerosol can only be detected in cloud-free regions. To make this clear, we added to the first paragraph of Sec. 4:

To verify our results we compared the MIPAS aerosol detections with SO_2 and ash detections by AIRS. Note that gas phase SO_2 is emitted by volcanic eruptions and conversion to liquid sulfate (H_2SO_4) starts immediately after injection into the atmosphere by oxidation (von Glasow et al., 2009).

P4394,L24: I don't think that a qualitative comparison of the location of SO2 and sulphate plumes can be registered as "perfect" agreement. e.g. the height of the SO2 is unknown compared to the sulfate and there is no model used linking formation of sulfate from SO2 so their respective concentrations cannot be compared.

We agree that "perfect" is not appropriate here. However, because the sulfate aerosol forms from the SO_2, it can be expected that both are in the same air masses. Our comparison is meant to show that there is a good agreement in the horizontal location of the detected fresh volcanic plume. Hence we rewrote in the first paragraph of Sec. 4:

For our comparisons of the horizontal plume locations we used the AIRS SO_2 index and the AIRS ash index by Hoffmann et al. (2014).

and in the second paragraph:

The SO_2 measured by AIRS is the precursor gas to sulfate aerosol measured by MIPAS. Since both, SO_2 and sulfate aerosol can be detected, the SO_2 oxidized

only partially during the six days after the eruption and the AIRS and MIPAS measurements agree well in location.

P4395,L13: Is the decay of SO2 consistent with the expected rate?

Yes. Usually the SO_2 lifetime in the troposphere is about 2 weeks when oxidation is the major depletion process (von Glasow et al., 2009). For reactions on cloud droplets depletion is even faster (hours to days) (von Glasow et al., 2009). Hence it can be expected that 4 weeks after the Grimsvötn eruption all SO_2 is gone. To substantiate this argument we rewrote this sentence:

It is expected that four weeks after this eruption the emitted SO_2 is completely oxidized and converted to sulfate aerosol (von Glasow et al., 2009) and hence, can no longer be seen in the AIRS SO_2 measurements (Hoffmann et al., 2016).

P4396,L7: Do you mean sulfur as in "sulfur budget" since MIPAS also measures SO2 and sulfate?

We mean sulfate aerosol. To clarify this point we rephrased the sentence:

However, in contrast to AIRS volcanic emission measurements (ash and SO_2) the MIPAS volcanic emission measurements (comprising SO_2 (Höpfner et al., 2013), ash (Griessbach et al., 2014), and sulfate aerosol (this study)) can trace volcanic emissions in the form of ash and sulfate aerosol for much longer time scales (e.g. from June 2011 until April 2012 in case of the Nabro eruption, not shown). This is due to a higher sensitivity of MIPAS to the aerosol and due to the fact that SO_2 is converted to sulfate aerosol on a timescale of about 4 weeks.

References

Ackerman, S. A.: Remote sensing aerosols using satellite infrared observations, J. Geophys. Res., 102, 17 069–17 079, doi:10.1029/96JD03066, 1997.

Ackerman, S. A., Smith, W. L., Spinhirne, J. D., and Revercomb, H. E.: The 27-28 October 1986 FIRE IFO cirrus case-study - spectral properties of cirrus clouds in the 8-12 μm window, Month. Weath. Rev., 118, 2377–2388, doi:10.1175/1520-0493(1990)118⟨2377:TOFICC⟩2.0.CO;2, 1990.

Baran, A., Foot, J., and Dibben, P.: Satellite detection of volcanic sulfuric-acid aerosol, Geophys. Res. Lett., 20, 1799–1801, doi:10.1029/93GL01965, 1993.

Bauman, J. J., Russell, P. B., Geller, M. A., and Hamill, P.: A stratospheric aerosol climatology from SAGE II and CLAES measurements: 2. Results and comparisons, 1984-1999, J. Geophys. Res., 108, 4383, doi:10.1029/2002JD002993, 2003.

Clarisse, L., Hurtmans, D., Prata, A. J., Karagulian, F., Clerbaux, C., De Maziere, M., and Coheur, P.-F.: Retrieving radius, concentration, optical depth, and mass of different types of aerosols from high-resolution infrared nadir spectra, Appl. Optics, 49, 3713–3722, 2010.

Clarisse, L., Coheur, P. F., Prata, F., Hadji-Lazaro, J., Hurtmans, D., and Clerbaux, C.: A unified approach to infrared aerosol remote sensing and type specification, Atmos. Chem. Phys., 13, 2195–2221, doi:10.5194/acp-13-2195-2013, 2013.

Clough, S., Shephard, M. W., Mlawer, E. J., Delamere, J. S., Iacono, M. J., Cady-Pereira, K., Boukabara, S., and Brown, P. D.: Atmospheric radiative transfer modeling: A summary of the AER codes, J. Quant. Spectrosc. Radiat. Transfer, 91, 233–244, 2005.

Davis, S., Hlavka, D., Jensen, E., Rosenlof, K., Yang, Q. O., Schmidt, S., Borrmann, S., Frey, W., Lawson, P., Voemel, H., and Bui, T. P.: In situ and lidar observations of tropopause subvisible cirrus clouds during TC4, J. Geophys. Res., 115, doi:10.1029/2009JD013093, 2010.

Dee, D. P., Uppala, S. M., Simmons, A. J., Berrisford, P., Poli, P., Kobayashi, S., Andrae, U., Balmaseda, M. A., Balsamo, G., Bauer, P., Bechtold, P.,

Beljaars, A. C. M., van de Berg, L., Bidlot, J., Bormann, N., Delsol, C., Dragani, R., Fuentes, M., Geer, A. J., Haimberger, L., Healy, S. B., Hersbach, H., Holm, E. V., Isaksen, L., Kallberg, P., Koehler, M., Matricardi, M., McNally, A. P., Monge-Sanz, B. M., Morcrette, J.-J., Park, B.-K., Peubey, C., de Rosnay, P., Tavolato, C., Thépaut, J.-N., and Vitart, F.: The ERA-Interim reanalysis: configuration and performance of the data assimilation system, Quart. J. Roy. Meteorol. Soc., 137, 553–597, doi:10.1002/qj.828, 2011.

Di Pierro, M., Jaeglé, L., Eloranta, E. W., and Sharma, S.: Spatial and seasonal distribution of Arctic aerosols observed by the CALIOP satellite instrument (2006–2012), Atmospheric Chemistry and Physics, 13, 7075–7095, doi:10.5194/acp-13-7075-2013, URL `http://www.atmos-chem-phys.net/13/7075/2013/`, 2013.

Fromm, M., Lindsey, D. T., Servranckx, R., Yue, G., Trickl, T., Sica, R., Doucet, P., and Godin-Beekmann, S. E.: The untold story of pyrocumulonimbus, Bull. Amer. Met. Soc., 91, 1193–1209, doi:10.1175/2010BAMS3004.1, 2010.

Fromm, M., Kablick, III, G., Nedoluha, G., Carboni, E., Grainger, R., Campbell, J., and Lewis, J.: Correcting the record of volcanic stratospheric aerosol impact: Nabro and Sarychev Peak, J. Geophys. Res., 119, 10,343–10,364, doi:10.1002/2014JD021507, 2014.

Gangale, G., Prata, A. J., and Clarisse, L.: The infrared spectral signature of volcanic ash determined from high-spectral resolution satellite measurements, Remote Sens. Environ., 114, 414–425, doi:10.1016/j.rse.2009.09.007, 2010.

Gille, J., Barnett, J., Arter, P., Barker, M., Bernath, P., Boone, C., Cavanaugh, C., Chow, J., Coffey, M., Craft, J., Craig, C., Dials, M., Dean, V., Eden, T., Edwards, D. P., Francis, G., Halvorson, C., Harvey, L., Hepplewhite, C., Khosravi, R., Kinnison, D., Krinsky, C., Lambert, A., Lee, H., Lyjak, L., Loh, J., Mankin, W., Massie, S., McInerney, J., Moorhouse, J., Nardi, B., Packman, D., Randall, C., Reburn, J., Rudolf, W., Schwartz, M., Serafin, J., Stone, K., Torpy, B., Walker, K., Waterfall, A., Watkins, R., Whitney, J., Woodard, D., and Young, G.: High Resolution Dynamics Limb Sounder: Experiment overview, recovery, and validation of initial

temperature data, J. Geophys. Res., 113, doi:10.1029/2007JD008824, URL http://dx.doi.org/10.1029/2007JD008824, d16S43, 2008.

Griessbach, S., Hoffmann, L., Hoepfner, M., Riese, M., and Spang, R.: Scattering in infrared radiative transfer: A comparison between the spectrally averaging model JURASSIC and the line-by-line model KOPRA, J. Quant. Spectrosc. Radiat. Transfer, 27, 102–118, doi:10.1016/j.jqsrt.2013.05.004, 2013.

Griessbach, S., Hoffmann, L., Spang, R., and Riese, M.: Volcanic ash detection with infrared limb sounding: MIPAS observations and radiative transfer simulations, Atmos. Meas. Tech., 7, 1487–1507, doi:10.5194/amt-7-1487-214, 2014.

Guehenneux, Y., Gouhier, M., and Labazuy, P.: Improved space borne detection of volcanic ash for real-time monitoring using 3-Band method, J. Volc. Geotherm. Res., 293, 25–45, doi:10.1016/j.jvolgeores.2015.01.005, 2015.

Hoffmann, L., Griessbach, S., and Meyer, C. I.: Volcanic emissions from AIRS observations: detection methods, case study, and statistical analysis, in: Proceedings of SPIE Volume 9242, Remote Sensing of Clouds and the Atmosphere XIX; and Optics in Atmospheric Propagation and Adaptive Systems XVII, SPIE Remote Sensing Europe, doi:10.1117/12.2066326, 2014.

Hoffmann, L., Rößler, T., Griessbach, S., Heng, Y., and Stein, O.: Lagrangian transport simulations of volcanic sulfur dioxide emissions: Impact of meteorological data products, J. Geophys. Res., 121, 4651–4673, doi:10.1002/2015JD023749, URL http://dx.doi.org/10.1002/2015JD023749, 2016.

Hong, G., Yang, P., Heidinger, A. K., Pavolonis, M. J., Baum, B. A., and Platnick, S. E.: Detecting opaque and nonopaque tropical upper tropospheric ice clouds: A trispectral technique based on the MODIS 8–12 μm window bands, J. Geophys. Res., 115, doi:10.1029/2010JD014004, URL http://dx.doi.org/10.1029/2010JD014004, d20214, 2010.

Höpfner, M., Pitts, M. C., and Poole, L. R.: Comparison between CALIPSO and MIPAS observations of polar stratospheric clouds, J. Geophys. Res., 114, D00H05, doi:10.1029/2009JD012114, 2009.

Höpfner, M., Glatthor, N., Grabowski, U., Kellmann, S., Kiefer, M., Linden, A., Orphal, J., Stiller, G., von Clarmann, T., Funke, B., and Boone, C. D.: Sulfur dioxide (SO_2) as observed by MIPAS/Envisat: temporal development and spatial distribution at 15–45 km altitude, Atmos. Chem. Phys., 13, 10 405–10 423, doi:10.5194/acp-13-10405-2013, URL http://www.atmos-chem-phys.net/13/10405/2013/, 2013.

Hu, Y., Rodier, S., Xu, K.-m., Sun, W., Huang, J., Lin, B., Zhai, P., and Josset, D.: Occurrence, liquid water content, and fraction of supercooled water clouds from combined CALIOP/IIR/MODIS measurements, J. Geophys. Res., 115, n/a–n/a, doi:10.1029/2009JD012384, URL http://dx.doi.org/10.1029/2009JD012384, d00H34, 2010.

Hurley, J., Dudhia, A., and Grainger, R. G.: Retrieval of macrophysical cloud parameters from MIPAS: algorithm description, Atmos. Meas. Tech., 4, 683–704, 2011.

Junge, C. E., Manson, J. E., and Chagnon, C. W.: A World-wide Stratospheric Aerosol Layer, Science, 133, 1478–1479, 1961.

Karagulian, F., Clarisse, L., Clerbaux, C., Prata, A. J., Hurtmans, D., and Coheur, P. F.: Detection of volcanic SO_2, ash, and H_2SO_4 using the Infrared Atmospheric Sounding Interferometer (IASI), J. Geophys. Res., 115, D00L02, doi:10.1029/2009JD012786, 2010.

Kent, G., Trepte, C., Wang, P., and Lucker, P.: Problems in separating aerosol and cloud in the Stratospheric Aerosol and Gas Experiment (SAGE) II data set under conditions of lofted dust: Application to the Asian deserts, J. Geophys. Res., 108, doi:10.1029/2002JD002412, 2003.

Klueser, L., Erbertseder, T., and Meyer-Arnek, J.: Observation of volcanic ash from Puyehue-Cordón Caulle with IASI, Atmos. Meas. Tech., 6, 35–46, doi:10.5194/amt-6-35-2013, 2013.

Klueser, L., Martynenko, D., and Holzer-Popp, T.: Thermal infrared remote sensing of mineral dust over land and ocean: a spectral SVD based retrieval approach for IASI, Atmos. Meas. Tech., 4, 757–773, doi:10.5194/amt-4-757-2011, 2011.

Klueser, L., Kleiber, P., Holzer-Popp, T., and Grassian, V. H.: Desert dust observation from space - Application of measured mineral component infrared extinction spectra, Atmos. Environment, 54, 419–427, doi: 10.1016/j.atmosenv.2012.02.011, 2012.

Liu, Z., Fairlie, T. D., Uno, I., Huang, J., Wu, D., Omar, A., Kar, J., Vaughan, M., Rogers, R., Winker, D., Trepte, C., Hu, Y., Sun, W., Lin, B., and Cheng, A.: Transpacific transport and evolution of the optical properties of Asian dust, J. Quant. Spectrosc. Radiat. Transfer, 116, 24 – 33, doi:http://dx.doi.org/10.1016/j.jqsrt.2012.11.011, URL http://www.sciencedirect.com/science/article/pii/S0022407312004979, 2013.

Massie, S., Gille, J., Khosravi, R., Lee, H., Kinnison, D., Francis, G., Nardi, B., Eden, T., Craig, C., Halvorson, C., Coffey, M., Packman, D., Cavanaugh, C., Craft, J., Dean, V., Ellis, D., Barnett, J., Hepplewhite, C., Lambert, A., Manney, G., Strawa, A., and Legg, M.: High Resolution Dynamics Limb Sounder observations of polar stratospheric clouds and subvisible cirrus, J. Geophys. Res., 112, doi:10.1029/2007JD008788, URL http://dx.doi.org/10.1029/2007JD008788, d24S31, 2007.

Mossop, S.: Volcanic dust collected at altitude of 20 km, Nature, 203, 824–827, doi:10.1038/203824a0, 1964.

Murphy, D. M., Cziczo, D. J., Hudson, P. K., and Thomson, D. S.: Carbonaceous material in aerosol particles in the lower stratosphere and tropopause region, J. Geophys. Res., 112, D04203, doi:10.1029/2006JD007297, 2007.

Peyridieu, S., Chédin, A., Tanré, D., Capelle, V., Pierangelo, C., Lamquin, N., and Armante, R.: Saharan dust infrared optical depth and altitude retrieved from AIRS: a focus over North Atlantic – and comparison to MODIS and CALIPSO, Atmos. Chem. Phys., 10, 1953–1967, doi:10.5194/acp-10-1953-2010, URL http://www.atmos-chem-phys.net/10/1953/2010/, 2010.

Prata, A.: Observations of volcanic ash clouds in the 10-12-mu-m window using AVHRR/2 data, Int. J. Remote Sensing, 10, 751–761, 1989a.

Prata, A.: Infrared radiative-transfer calculations for volcanic ash clouds, Geophys. Res. Lett., 16, 1293–1296, doi:10.1029/GL016i011p01293, 1989b.

Remedios, J. J., Leigh, R. J., Waterfall, A. M., Moore, D. P., Sembhi, H., Parkes, I., Greenhough, J., Chipperfield, M., and Hauglustaine, D.: MIPAS reference atmospheres and comparisons to V4.61/V4.62 MIPAS level 2 geophysical data sets, Atmos. Chem. Phys. Discuss., 7, 9973–10 017, 2007.

Rieger, L. A., Bourassa, A. E., and Degenstein, D. A.: Merging the OSIRIS and SAGE II stratospheric aerosol records, J. Geophys. Res., 120, 8890–8904, doi:10.1002/2015JD023133, URL http://dx.doi.org/10.1002/2015JD023133, 2015JD023133, 2015.

Roberts, R. E., Selby, J. E. A., and Biberman, L. M.: Infrared continuum absorption by atmospheric water vapor in the 8–12-μm window, Appl. Optics, 15, 2085–2090, doi:10.1364/AO.15.002085, URL http://ao.osa.org/abstract.cfm?URI=ao-15-9-2085, 1976.

Sembhi, H., Remedios, J., Trent, T., Moore, D. P., Spang, R., Massie, S., and Vernier, J. P.: MIPAS detection of cloud and aerosol particle occurrence in the UTLS with comparison to HIRDLS and CALIOP, Atmos. Meas. Tech., 5, 2537–2553, doi:10.5194/amt-5-2537-2012, 2012.

Spang, R., Remedios, J. J., and Barkley, M. P.: Colour indices for the detection and differentiation of cloud type in infra-red limb emission spectra, Adv. Space Res., 33, 1041–1047, 2004.

Spang, R., Günther, G., Riese, M., Hoffmann, L., Müller, R., and Griessbach, S.: Satellite observations of cirrus clouds in the Northern Hemisphere lowermost stratosphere, Atmos. Chem. Phys., 15, 927–950, doi:10.5194/acp-15-927-2015, URL http://www.atmos-chem-phys.net/15/927/2015/, 2015.

Thomason, L., Poole, L., and Deshler, T.: A global climatology of stratospheric aerosol surface area density deduced from stratospheric aerosol and gas experiment II measurements: 1984-1994, J. Geophys. Res., 102, 8967–8976, doi:10.1029/96JD02962, 1997.

Thomason, L. W.: Toward a combined SAGE II–HALOE aerosol climatology: an evaluation of HALOE version 19 stratospheric aerosol extinction coefficient observations, Atmos. Chem. Phys., 12, 8177–8188, doi:10.5194/acp-12-8177-2012, 2012.

Thomason, L. W. and Vernier, J. P.: Improved SAGE II cloud/aerosol categorization and observations of the Asian tropopause aerosol layer: 1989-2005, Atmos. Chem. Phys., 13, 4605–4616, doi:10.5194/acp-13-4605-2013, 2013.

Timofeyev, Y. M., Kostsov, V., and Grassl, H.: Numerical investigations of the accuracy of the remote sensing of non-LTE atmosphere by space-borne spectral measurements of limb i.r. radiation: 15 μm CO_2 bands, 9.6 μm O_3 bands and 10 μm CO_2 laser bands, J. Quant. Spectrosc. Radiat. Transfer, 53, 613 – 632, doi:10.1016/0022-4073(95)00025-G, URL `http://www.sciencedirect.com/science/article/pii/002240739500025G`, 1995.

Vernier, J. P., Thomason, L. W., Pommereau, J. P., Bourassa, A., Pelon, J., Garnier, A., Hauchecorne, A., Blanot, L., Trepte, C., Degenstein, D., and Vargas, F.: Major influence of tropical volcanic eruptions on the stratospheric aerosol layer during the last decade, Geophys. Res. Lett., 38, L12807, doi:10.1029/2011GL047563, 2011.

von Glasow, R., Bobrowski, N., and Kern, C.: The effects of volcanic eruptions on atmospheric chemistry, Chemical Geology, 263, 131–142, doi:10.1016/j.chemgeo.2008.08.020, 2009.

Weigel, R., Volk, C. M., Kandler, K., Hösen, E., Günther, G., Vogel, B., Grooß, J.-U., Khaykin, S., Belyaev, G. V., and Borrmann, S.: Enhancements of the refractory submicron aerosol fraction in the Arctic polar vortex: feature or exception?, Atmos. Chem. Phys., 14, 12 319–12 342, doi:10.5194/acp-14-12319-2014, URL `http://www.atmos-chem-phys.net/14/12319/2014/`, 2014.

Zängl, G. and Hoinka, K.: The tropopause in the polar regions, J. Clim., 14, 3117–3139, doi:10.1175/1520-0442(2001)014⟨3117:TTITPR⟩2.0.CO;2, 2001.